EFFECTS OF VARIABLE VISCOSITY AND THERMAL CONDUCTIVITY ON NATURAL-CONVECTION OF NANOFLUIDS PAST A VERTICAL PLATE IN POROUS MEDIA

A. Noghrehabadi * **M. Ghalambaz** **A. Ghanbarzadeh**

Department of Mechanical Engineering
Shahid Chamran University of Ahvaz
Ahvaz, Iran

ABSTRACT

The effects of variable viscosity and thermal conductivity on the natural convection heat transfer over a vertical plate embedded in a porous medium saturated by a nanofluid are investigated. In the nanofluid model, a gradient of nanoparticles concentration because of Brownian motion and thermophoresis forces is taken into account. The nanofluid viscosity and the thermal conductivity are assumed as a function of local nanoparticles volume fraction. The appropriate similarity variables are used to convert the governing partial differential equations into a set of highly coupled nonlinear ordinary differential equations, and then, they numerically solved using the Runge-Kutta-Fehlberg method. The practical range of non- dimensional parameters is discussed. The results show that the range of Lewis number as well as Brownian motion and thermophoresis parameters which were used in previous studies should be reconsidered. The effect of non-dimensional parameters on the boundary layer is examined. The results show that the reduced Nusselt number would increase with increase of viscosity parameter and would decrease with increase of thermal conductivity parameter.

Keywords: Natural-convection, Variable viscosity, Variable thermal conductivity, Nanofluids, Porous media.

1. INTRODUCTION

Due to many industrial applications, *e.g.* for example high performance cooling systems where energy-efficient heat transfer fluids are crucial, improving the performance of cooling systems have been widely demanded by the industry. The key problem here, which has involved many researchers and engineers, is to find economically affordable ways for improving the conventional cooling systems. The challenge, though, is that the inherently low thermal conductivity of fluids is a primary limitation against developing highly efficient cooling systems. Considering high thermal conductivity of metallic solids and their oxides, the idea of dispersing solid particles in the fluid flow was developed to enhance the overall fluid conductivity. In 1881, this idea was implemented through dispersing micro and millimeter sized particles in base fluids. However, due to stability problems, sedimentation and clogging the channels, the fluids containing small scale particles did not turn out to be economic. Recently, nanofluids are proposed to resolve the latter limitation [1]. Nanofluids are synthesis by suspending nanoparticles, *i.e.* metallic or nonmetallic particles of nanometer dimensions, in the traditional heat transfer fluids such as water, oil, or ethylene glycol [1]. The most important characteristic of nanofluids is their high thermal conductivity relative to the base fluids, which can be achieved even at very low volume fraction of nanoparticles. The nanofluids can flow smoothly through microchannels without clogging them, because they are small enough to behave similar to liquid molecules [2]. This unique property of nanofluids in enhancement of heat transfer has attracted many researchers to investigate the heat transfer characteristics of nanofluids [3-5]. Many researchers reported that the presence of the nanoparticles in the base fluid tremendously enhances the effective thermal conductivity of the fluid and consequently enhances the heat transfer characteristics [1,6-8]. The heat transfer enhancement of nanofluids then became a means for surpassing the limited heat transfer performance of available liquids.

Convective flow in porous media has a wide range of engineering applications, such as solar energy collectors, heat exchangers, geothermal and hydrocarbon recovery, groundwater systems for agricultural usages and flow through filtering media [9-13]. That is why there are numerous studies reported on convective flow in porous media.

Natural convection flow in porous media is extensively studied in the literature. For example, similarity solution of natural convection boundary layer flow along a vertical plate with variable wall temperature was investigated by Cheng and Minkowycz [14].

* Corresponding author (noghrehabadi@scu.ac.ir)

DOI : 10.1017/jmech.2013.61

They reported that the temperature and velocity profiles of a Darcy flow are identical. Likewise, the problem of free convection from a vertical plate with non-uniform surface temperature was studied by Gorla and Zinalabedini in 1987 [15]. Joshi and Gebhart [16] studied the mixed convection in porous media adjacent to a vertical uniform heat flux surface. Belhachmi *et al*. [17] simulated the free convection heat transfer about a vertical flat plate embedded in a porous medium. They presented some experimental results along with physical models for validating their numerical simulations.

Due to the unique thermal properties of nanofluids and their exclusive role in enhancing the heat transfer, researchers have dedicated a lot of efforts to study the influence of nanoparticles on the heat transfer of nanofluids. It is believed that several slip mechanisms are involved in the convection of nanofluids, and thus the volume fraction of nanoparticles in the nanofluid may not be uniform. The consideration of additional heat transfer mechanisms in the convective heat transfer of nanofluids was further developed by Buongiorno [18]. He discussed seven possible mechanisms, during convection of nanofluids, being inertia, Brownian diffusion, thermophoresis, diffusionphoresis, Magnus effect, fluid drainage, and gravity for particles slips. Among the investigated mechanisms, the thermophoresis and the Brownian diffusion were found to be important.

Few studies were performed in association with the natural convection of nanofluids using models including slip mechanisms. Nield and Kuznetsov [19] studied the classical Cheng-Minkowycz problem for natural convective boundary-layer flow in a porous medium saturated with a nanofluid. They found that the reduced Nusselt number is a decreasing function of both Brownian motion and thermophoresis parameters. Later, Chamkha *et al.* [20] presented a non-similar solution for natural convective boundary layer flow over a sphere embedded in a porous medium saturated with a nanofluid. Rashad *et al.* [21] investigated natural convection boundary layer of a nanofluid about a permeable vertical full cone embedded in a saturated porous medium. Moreover, natural convective boundary layer flow over a horizontal plate embedded in a porous medium saturated with a nanofluid was investigated by Gorla and Chamkha [22]. Mixed convective boundary layer flow over a vertical wedge embedded in a porous medium saturated with a nanofluid has been analyzed by Gorla *et al.* [13].

In all above-mentioned studies, [13,19-22], it was assumed that the thermal properties of the nanofluid, *i.e*. thermal conductivity and viscosity, are constant and no efforts have been made to study the effect of variable thermal conductivity and variable viscosity. However, it has been reported that the thermo-physical properties of nanofluids are strongly affected by volume fraction of nanoparticles [1,23,24]. Moreover, the appropriate range of Brownian motion parameter, thermophoresis parameter, buoyancy ratio parameter and Lewis number has not been discussed in previous researches.

In the present study, the thermal conductivity and viscosity of nanofluid are assumed to vary as a function of local nanoparticle volume fraction. Therefore, two new parameters, namely variable thermal conductivity parameter and variable viscosity parameter are introduced. In addition, the practical range of non-dimensional nanofluid parameters is discussed. The results show that the range of these parameters which has been used by previous researchers should be reconsidered. According to the author's knowledge, the influence of local volume fraction of nanoparticles on the viscosity and thermal conductivity of nanofluids has not been considered by the previous researchers.

2. FORMULATION OF THE PROBLEM

Consider the two-dimensional steady natural convection boundary layer flow past a vertical plate placed in a Darcy porous medium saturated with nanofluid. The plate surface is imposed to a constant temperature T_w. The coordinate system is chosen such that x-axis is aligned with the flow on the surface of the plate. A schematic of the physical model and coordinate system are shown in Fig. 1. As shown in Fig. 1, there are three distinct boundary layers namely, hydrodynamic boundary layer, thermal boundary layer and nanoparticle concentration boundary layer. It is assumed that the nanoparticle volume fraction (φ) at the wall surface ($y = 0$) has a fixed value of φ_w. The ambient values of T and φ, as y tends to infinity, are denoted by T_∞ and φ_∞, respectively. The flow in the porous medium with porosity ε and permeability K is considered as Darcy flow, and the Oberbeck-Boussinesq approximation is applied. Furthermore, it is assumed that the porous medium is homogeneous and in local thermal equilibrium.

Following the work of Nield and Kuznetsov [19] and applying the standard boundary layer approximations, the steady-state conservation of total mass (Eq. (1)), momentum (Eq. (2b)), and energy (Eq. (3)) as well as conservation of nanoparticles (Eq. (4)) for nanofluids in the presence of variable properties of nanofluid (nanofluid viscosity and thermal conductivity) are as follows,

$$\frac{\partial u}{\partial x}+\frac{\partial v}{\partial y}=0\,, \tag{1}$$

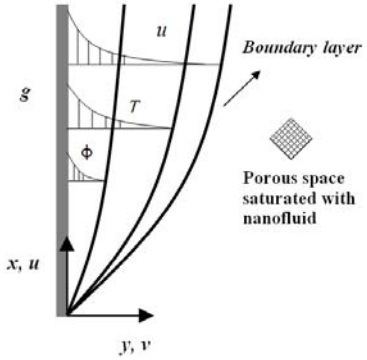

Fig. 1 Schematic view and the coordinate systems utilized to model convective heat transfer past a vertical plate placed inside a homogeneous porous medium saturated with a nanofluid

https://doi.org/10.1017/jmech.2013.61 Published online by Cambridge University Press

$$\frac{\partial p}{\partial y}=0\,, \tag{2a}$$

$$\frac{\mu(\phi)}{K}u=\left[-\left(\frac{\partial p}{\partial x}-(1-\phi_\infty)\,\beta g\rho_{f_\infty}(T-T_\infty)\right)\right.$$
$$\left.-(\rho_P-\rho_{f_\infty})g(\phi-\phi_\infty)\right], \tag{2b}$$

$$\frac{\partial\psi}{\partial y}\frac{\partial T}{\partial x}-\frac{\partial\psi}{\partial x}\frac{\partial T}{\partial y}=\frac{1}{(\rho c)_f}\frac{\partial}{\partial y}\left(k_m(\phi)\frac{\partial T}{\partial y}\right)$$
$$+\tau\left[D_B\frac{\partial\phi}{\partial y}\frac{\partial T}{\partial y}+\frac{D_T}{T}\left(\frac{\partial T}{\partial y}\right)^2\right] \tag{3}$$

$$\frac{1}{\varepsilon}\left[u\frac{\partial\phi}{\partial x}+v\frac{\partial\phi}{\partial y}\right]=D_B\frac{\partial^2\phi}{\partial y^2}+\left(\frac{D_T}{T_\infty}\right)\frac{\partial^2 T}{\partial y^2}\,, \tag{4}$$

τ, in the above equations, is defined as:

$$\tau=\frac{\varepsilon(\rho c)_p}{(\rho c)_f}\,, \tag{5}$$

Based on the problem description, the boundary conditions are:

$$v=0\,,\quad T=T_w\,,\quad \phi=\phi_w\,,\quad \text{at}\quad y=0\,,\ x\geq 0 \tag{6}$$

$$u=v=0\,,\quad T\to T_\infty\,,\quad \phi\to\phi_\infty\,,\quad \text{at}\quad y\to\infty \tag{7}$$

In many studies [25-30], the viscosity and thermal conductivity of fluid were presumed to be a function of fluid temperature. In the latter studies, the fluid was considered as pure. In this study, however, a nanofluid is considered as the working fluid. The reviews of experimental reports reveal that the viscosity and thermal conductivity of nanofluids are strongly dependent on the volume fraction of nanoparticles rather than the temperature [1,23,24]. Therefore, the thermal conductivity and viscosity of the nanofluid are considered as a function of local volume fraction of nanoparticles. To aim this purpose, the nanofluid viscosity and thermal conductivity are assumed as a reciprocal and a linear function of local nanoparticle volume fraction, respectively. Therefore, the viscosity can be written as

$$\frac{1}{\mu}=\frac{1}{\mu_\infty}\left(1+\gamma(\phi-\phi_\infty)\right) \tag{8}$$

Equation (8) can be further simplified as

$$\frac{1}{\mu}=m_\mu(\phi-\phi_r) \tag{9}$$

where m_μ and φ_r given by

$$m_\mu=\frac{\gamma}{\mu_\infty}\,,\quad \phi_r=\phi_\infty-\frac{1}{\gamma} \tag{10}$$

In Eqs. (8) and (9), γ, μ_∞, φ_∞, m_μ and φ_r are constant. In addition, the nanoparticle volume fraction-dependent thermal conductivity is introduced as

$$k_m(\phi)=k_{m,\infty}\left(1+m_k(\phi-\phi_\infty)\right) \tag{11}$$

where, φ_w, φ_∞ and m_k are constant, and $m_k = Nc / (\varphi_w - \varphi_\infty)$. Here, Nc is the variable thermal conductivity parameter and $k_{m,\infty}$ is the effective thermal conductivity of porous medium and nanofluid outside the boundary layers.

Equations (2a) and (2b) are simplified using cross-differentiation, and the continuity equation will also be satisfied by introducing a stream function, (ψ):

$$u=\frac{\partial\psi}{\partial y}\,,\quad v=-\frac{\partial\psi}{\partial x}\,, \tag{12}$$

By substituting Eqs. (9), (11) and (12) in Eqs. (2b) and (3) and simplifying the resulting expression, the governing differential equations (Eqs. (1) ~ (4)) are then reduced to the following three equations,

$$\frac{1}{K}\left(\frac{\partial\left(\frac{1}{m_\mu(\phi-\phi_r)}\right)}{\partial y}\frac{\partial\psi}{\partial y}+\frac{1}{m_\mu(\phi-\phi_r)}\cdot\frac{\partial^2\psi}{\partial y^2}\right)$$
$$=\left[(1-\phi_\infty)\,\beta g\rho_{f_\infty}\frac{\partial T}{\partial y}-(\rho_P-\rho_{f_\infty})g\frac{\partial\phi}{\partial y}\right] \tag{13}$$

$$\frac{\partial\psi}{\partial y}\frac{\partial T}{\partial x}-\frac{\partial\psi}{\partial x}\frac{\partial T}{\partial y}=\frac{1}{(\rho c)_f}\frac{\partial}{\partial y}\left[k_{m,\infty}\left(1+\frac{Nc}{(\phi_w-\phi_\infty)}(\phi-\phi_\infty)\right)\frac{\partial T}{\partial y}\right]$$
$$+\tau\left[D_B\frac{\partial\phi}{\partial y}\frac{\partial T}{\partial y}+\frac{D_T}{T_\infty}\left(\frac{\partial T}{\partial y}\right)^2\right] \tag{14}$$

$$\frac{1}{\varepsilon}\left(\frac{\partial\psi}{\partial y}\frac{\partial\phi}{\partial x}-\frac{\partial\psi}{\partial x}\frac{\partial\phi}{\partial y}\right)=D_B\frac{\partial^2\phi}{\partial y^2}+\left(\frac{D_T}{T_\infty}\right)\frac{\partial^2 T}{\partial y^2} \tag{15}$$

Here, the local Rayleigh number (Ra_x) is defined as [19],

$$Ra_x=\frac{(1-\phi_\infty)\rho_{f\infty}\beta Kgx(T_w-T_\infty)}{\mu_\infty\,\alpha_m} \tag{16}$$

To simplify the system of governing equations (Eqs. (13) ~ (15)) subject to the boundary conditions (Eqs. (6) and (7)), the similarity variable η is defined as,

$$\eta=\frac{y}{x}Ra_x^{\frac{1}{2}} \tag{17}$$

and the dimensionless similarity quantities S, f, Nv and θ as,

$$S=\frac{\psi}{\alpha_m Ra_x^{\frac{1}{2}}}\,,\quad f=\frac{\phi-\phi_\infty}{\phi_w-\phi_\infty}\,,\quad Nv=\frac{\phi_r-\phi_\infty}{\phi_w-\phi_\infty}\,,\quad \theta=\frac{T-T_\infty}{T_w-T_\infty} \tag{18}$$

https://doi.org/10.1017/jmech.2013.61 Published online by Cambridge University Press

Using the similarity variables, Eqs. (13) ~ (15) are reduced to the following three ordinary differential equations,

$$\frac{Nv}{(Nv-f)}S''+\frac{Nv.f'}{(Nv-f)^2}S'-\theta'+Nr.f'=0 \tag{19}$$

$$(1+Nc.f)\theta''+\frac{1}{2}.S\theta'+Nc.f'.\theta'+Nb.f'.\theta'+Nt(\theta')^2=0 \tag{20}$$

$$f''+\frac{1}{2}.Le.S.f'+\frac{Nt}{Nb}\theta''=0 \tag{21}$$

subject to the following boundary conditions,

$$\eta=0:\ S=0,\quad \theta=1,\quad f=1 \tag{22a}$$

$$\eta\to\infty:\ S'=0,\quad \theta=0,\quad f=0 \tag{22b}$$

where the non-dimensional parameters are as follow:

$$Nr=\frac{(\rho_p-\rho_{f\infty})(\phi_w-\phi_\infty)}{(1-\phi_\infty)\rho_{f\infty}\beta(T_w-T_\infty)},\quad Nb=\frac{\varepsilon(\rho c)_p D_B(\phi_w-\phi_\infty)}{(\rho c)_f\alpha_m},$$
$$Nt=\frac{\varepsilon(\rho c)_p D_T(T_w-T_\infty)}{(\rho c)_f\alpha_m T_\infty},\quad Le=\frac{\alpha_m}{\varepsilon D_B},$$
$$Nv=\frac{\phi_r-\phi_\infty}{\phi_w-\phi_\infty}=-\frac{1}{\gamma(\phi_w-\phi_\infty)} \tag{23}$$

Here, *Nr*, *Nb*, *Nt*, *Le*, *Nv* and *Nc* denote the buoyancy ratio parameter, the Brownian motion parameter, the thermophoresis parameter, the Lewis number, the variable thermal conductivity parameter and the variable viscosity parameter, respectively. It is worth mentioning that $Nv\to\infty$ and $Nc=0$ reduce the present study to the model of constant viscosity and constant thermal conductivity which was previously analyzed by Nield and Kuznetsov [19]. Furthermore, in this case (*i.e.* $Nv\to\infty$ and $Nc=0$), Eqs. (19) and (20) reduces to

$$S''-\theta'+Nr.f'=0 \tag{24}$$

$$\theta''+\frac{1}{2}.S\theta'+Nb.f'.\theta'+Nt(\theta')^2=0 \tag{25}$$

where are in good agreement with the equations reported by Nield and Kuznetsov [19].

It is interesting that integrating Eq. (19) once results in,

$$\frac{Nv}{(Nv-f(\eta))}S'(\eta)-\theta(\eta)+Nr.f(\eta)=C \tag{26a}$$

where *C* is a constant value which comes from the integration. Using boundary conditions of Eq. (22b) shows that the value of *C* is zero. Moreover, it is found that by using Eq. (26a) and implementing boundary conditions of Eq. (22a), the values of non-dimensional velocity on the wall as a function of *Nr* and *Nv* can be easy obtained as follow,

$$S'(0)=\frac{(Nv-1)(1-Nr)}{Nv} \tag{26b}$$

Equation (26b) demonstrates that the value of the non-dimensional surface velocity is only a function of the buoyancy ratio parameter *Nr* and variable viscosity parameter *Nv*. It is worth mentioning that in the case of fluid flow with constant viscosity ($Nv\to\infty$), the value of non-dimensional velocity on the wall is just directly related to the buoyancy ratio parameter *Nr*.

The quantities of local Nusselt number (Nu_x) and local Sherwood number (Sh_x), interested in thermal engineering design of industrial equipment, are defined as [19],

$$Nu_x=\frac{q_w x}{k(T_w-T_\infty)},\quad Sh_x=\frac{q_m x}{D_B(\phi_w-\phi_\infty)}, \tag{27}$$

Here, the quantities of q_w and q_m are the wall heat and mass fluxes, respectively. Using the similarity variables, the reduced Nusselt number (Nu_r) and reduced Sherwood number (Sh_r)are obtained as,

$$Nu_r=Ra_x^{\frac{-1}{2}}Nu_x=-\theta'(0),\quad Sh_r=Ra_x^{\frac{-1}{2}}Sh_x=-f'(0) \tag{28}$$

2.1 Physical Range of Parameters

In order to perform a realistic analysis on the effect of non-dimensional parameters on the flow, heat and mass transfer in the boundary layer, the practical range of nanofluid parameters should be clarified. To aim this purpose, first, the practical range of physical properties (*i.e.* D_B, D_T, $(\rho c)_p/(\rho c)_f$, β, α_m, *etc.*) should be analyzed.

For the water base nanofluids at room the temperature with nanoparticles of 100 nm diameters, the Brownian diffusion coefficient (D_B) ranges from 1×10^{-10} to 1×10^{-12}m^2/s [18]. The thermophoresis coefficient (D_T) also ranges from 1×10^{-10} to 1×10^{-12} [18,31]. The ranges of 5 to 40, 0 to 0.1 and 0 to 1 are considered for the temperature difference, the nanoparticle volume fraction difference and the porosity of porous medium, respectively. In order to evaluate the amount of remaining thermo-physical properties in the nanofluid parameters (*i.e.* $(\rho c)_p/(\rho c)_f$, $\rho_{f\infty}$, $\rho_p-\rho_f$, β and α_m), three different types of base fluids (water, oil and ethylene glycol) and two types of nanoparticles (Cu and Al_2O_3), which mostly have been used in the synthesis of nanofluids, are adopted. Therefore, the nanofluids are Cu-H_2O, Cu-Oil, Cu-$C_2H_4(OH)_4$, Al_2O_3-H_2O, Al_2O_3-Oil and Al_2O_3-$C_2H_4(OH)_4$. The thermo-physical properties of the base fluids and the nanoparticles are given in Table 1. These thermo-physical properties have been previously used by Oztop and Abu-Nada [32]. Based on the Table 1 and the work of Buongiorno [18], the thermo-physical range of parameters can be summarized in Table 2.

Now, the ranges of thermo-physical properties in the nanofluid parameters have been identified. By substituting minimum and maximum values of the thermo-physical properties into definition of nanofluid parameters, Eq. (23), the practical range of these parameters is obtained and summarized in Table 3. In the present study, we are interested in the case in which heat transfer is driving the flow rather than the mass transfer.

https://doi.org/10.1017/jmech.2013.61 Published online by Cambridge University Press

Therefore, the value of buoyancy-ratio parameter (*Nr*) is assumed very small (*Nr* << 1).

In the literature [13,19-22], for example, in the work of Nield and Kuznetsov [19], Gorla *et al.* [13] and Gorla and Chamkha [22], the range of 0.1 to 0.5 has been chosen for nanofluid parameters (*i.e. Nb*, *Nt* and *Nr*) to analyze the effect of these parameters on the boundary layer heat and mass transfer. In addition, they [13,19,22] have considered the range of 1 to 1000 for Lewis number. Moreover, Chamkha *et al.* [20] have chosen the range of 0.1 to 0.5 for *Nr*, *Nb* and *Nt* and the range of 1 to 100 for *Le*. Rashad *et al.* [21] have also adopted the range of 0.1 to 0.7 for *Nb*, *Nt*, *Nr* and the range of 1 to 100 for *Le*. However, the present analysis reveals that the range of nanofluid parameters in the previous works ([13,19-22]) should be reconsidered.

In order to demonstrate the range of variable viscosity parameter (*Nv*), the range of proportionality coefficient (γ) should be revealed. Based on Eq. (8), the value of γ is dependent on the values of uniform viscosity (μ_∞) and local viscosity (μ). Therefore, it is assumed that nanofluid has a uniform nanoparticles concentration (φ_∞) that is equal to 0.05. Four different models [6], including: Einstain, Brinkman, Batchelor and Saito, are adopted to determine the uniform viscosity (μ_∞) and local viscosity (μ). The details of these models can be found in [6]. The range of local volume fraction of nanoparticles (φ) is selected between 0 to 0.1. Then, the proportionality factor (γ) is evaluated using curve fitting. It is found that Eq. (8), using appropriate value of γ, is capable to estimate the values of local viscosity as a function of local volume fraction. The proportionality coefficient (γ) is evaluated for different nanofluids. The results show that γ varies between –2.0 to –3.0.

The values of γ are negative, and thereby, the values of *Nv* are positive. According to the Eq. (23) and the obtained range of γ, the values of variable viscosity parameter (*Nv*) are chosen to be in the range of $2 < Nv < \infty$ to clearly show the effect of this parameter on the dimensionless quantities. By selecting this wide range, the results obviously demonstrate the behavior of variable viscous fluid flow (*i.e.* $Nv = 2, 10, 20, 200$) and fluid flow with constant viscosity (*i.e.* $Nv \to \infty$). Likewise, For clarifying the values of variable thermal conductivity parameter (*Nc*), based on Eq. (11), it is necessary to determine the uniform effective thermal conductivity of porous medium ($k_{m,\infty}$) and the local effective thermal conductivity of porous medium (k_m). Therefore, four different models [6,33,34], namely, Hamilton-cylinders, Ya and Choi, Maxwell and Hamilton-spheres are considered to determine $k_{m,\infty}$ and k_m. considering the properties of various nanofluids and porous media (present in Table 1), the calculations were performed for different nanofluids and porous media. The results show that the effect of porous medium on the effective thermal conductivity and m_k is significant. The uniform nanoparticle concentration (φ_∞) is assumed equal to 0.05, and the range of local volume fraction of nanoparticles (φ) is selected between 0 to 0.1. Then, the proportionality factor (m_k) is evaluated using curve fitting. The results show that using the appropriate value of m_k provides excellent agreement between Maxwell model and Eq. (11) for different types of porous media. Repeating the calculations for different types of nanofluids and porous media demonstrates that the m_k ranges from 0 to 5. Therefore, in the present study, the parameter of *Nc* has been selected between 0 and 1 in order to cover the estimated range of this parameter.

Table 1 Thermo-physical properties of base fluids, nanoparticles [32] and porous media [9]

Physical properties	k (W/m.K)	ρ (kg/m^3)	C_p (J/kg.K)	β (K^{-1})	ε
Fluid phase (Water)	0.613	997.1	4179	21×10^{-5}	–
Fluid phase (Oil)	0.145	884.1	1909	70×10^{-5}	–
Fluid phase (Ethylene glycol)	0.252	1114.4	2415	65×10^{-5}	–
Cu	401	8933	385	1.67×10^{-5}	–
Al_2O_3	40	3970	765	0.85×10^{-5}	–
Porous phase (Sand)	3.0	–	–	–	0.45
Porous phase (Limestone)	1.26	–	–	–	0.04
Porous phase (Glass)	0.17	–	–	–	0.9

Table 2 The range of physical properties in definition of nanofluid parameters

Physical properties	Range of variation
$(\rho c)_p / (\rho c)_f$	0.73 to 1.996
$\rho_{f\infty}$	884.1 to 1114.4
$\rho_p - \rho_f$	2.8E+3 to 8E+3
β	21E−5 to 70E−5
α_m	1.94E−7 to 2.94E−7
D_B	1.0E−10 to 1.0E−12
D_T	1.0E−10 to 1.0E−12

Table 3 The range of nanofluid parameters, *i.e. Nb*, *Nc*, *Nr*, *Nt* and *Le*

Parameters	Range of variation
Nb	2.4E−9 to 1E−4
Nc	0 to 1.0
Nr	0 to +9.7E+2
Nt	4E−9 to 1.3E−4
Nv	2 to ∞
Le	1E+3 to 3E+6

3. NUMERICAL PROCEDURE

The system of Eqs. (19) ~ (21) subject to the boundary conditions (Eqs. (22a) and (22b)) is numerically

https://doi.org/10.1017/jmech.2013.61 Published online by Cambridge University Press

solved using an efficient, iterative fourth-order Runge-Kutta-Fehlberg method starting with an initial guess. In this method, every n^{th}-order equation is converted to n first order differential equations. Therefore, the system of high order ordinary differential equations is converted into a system of first order nonlinear differential equations. An iteration method is then applied on the latter system. A maximum relative error of 10^{-5} is used as the stopping criteria for the iterations. An important criterion for the success of this numerical approach is to choose an appropriate finite value of η_∞. Thus, in order to estimate the realistic value of η_∞, the solution process was started with initial guess value of $\eta_\infty = 6$. The value of η_∞ was updated and the solution process was repeated until further changes (increment) in η_∞ did not lead to any changes in the values of results or, in other words, the results are independent of the value of η_∞. The results show that the choice of $\eta_{max} = 10$ guarantees that all numerical solutions approach to their asymptotic values.

3.1 Code Validation

The case of $Nv \to \infty$ and $Nc = 0$ simulates the natural convection of constant thermal conductivity and viscosity flow over an isothermal flat plate embedded in a porous medium saturated with a nanofluid which recently has been analyzed by Nield and Kuznetsov [19]. Therefore, a comparison has been done between the present results and those reported by Nield and Kuznetsov [19] in a case in which $Nr = Nb = Nt = 0.5$, $Le = 10$, $Nc = 0$ and $Nv \to \infty$. The results of this comparison are illustrated in Fig. 2. As seen, this figure depicts good agreement between the present results and the previous study. In the work of Cheng and Minkowycz [14] for the case of pure fluid is has been reported that the non-dimensional temperature and velocity profiles are identical; however, Fig. 2 shows that the temperature and velocity profile are not identical because of the concentration gradient.

4. RESULTS AND DISCUSSION

The system of equations, *i.e.* Eqs. (19) ~ (21), subject to the boundary conditions, *i.e.* Eqs. (22a) and (22b), is numerically solved for selected values of buoyancy ratio parameter, Brownian motion parameter, thermophoresis parameter, variable thermal conductivity parameter and variable viscosity parameter.

The values of reduced Nusselt number ($-\theta'(0)$) and the values of reduced Sherwood number ($-f'(0)$) are shown in Table 4 for selected combination of *Nt*, *Nb*, *Nr*, *Nv* and *Nc* and for two selected values of $Le = 1E + 3$ and $Le = 2E + 3$. Table 4 clearly depicts that increase of variable viscosity parameter (*Nv*) would increase the magnitude of reduced Nusselt and sherwood numbers for two values of $Le = 1E + 3$ and $Le = 2E + 3$. Likewise, increase of variable thermal conductivity parameter tends to decrease the magnitude of reduced Nusselt number whereas increase the magnitude of Sherwood number. This table reveals that the increase of thermophoresis parameter does not show any significant effect on the reduced Nusselt number. In addition, increase of Brownian motion parameter (or buoyancy ratio parameter) increases (or decreases) the reduced Nusselt number. Nield and Kuznetsov [19], using curve fitting, obtained a relation between the reduced Nusselt number and nanofluid parameters (*i.e. Nt, Nb* and *Nr*) in the case of $Le = 10$. However, the results of present study do not confirm the results which were reported by Nield and Kuznetsov [19]. Despite of present results, they found a decreasing trend for the reduced Nusselt number by increase of thermophoresis and Brownian motion parameters. This difference is due to the fact that a different physical range of parameters have been chosen in the work of Nield and Kuznetsov [19].

Table 4 shows that the most significant parameter which affects the reduced Nusselt number is the variable thermal conductivity parameter (*Nc*). However, the influence of other non-dimensional parameters on the reduced Nusselt number is comparatively insignificant. Therefore, it can be concluded that the heat transfer associated via diffusion of nanoparticles is negligible compared with heat transfer associated via conduction and convection.

Figures 3 and 4 depict the effect of variable viscosity parameter (*Nv*) on the dimensionless velocity, temperature and concentration profiles. In preparing these figures, the values of *Nr*, *Nb*, *Nt*, *Nc* and *Le* are kept constant. These figures illustrate that the thickness of concentration boundary layer is very small in comparison with hydrodynamic and thermal boundary layers. Therefore, the results are plotted in the logarithmic scale to clearly show the effect of variable viscosity parameter on the boundary layers. Figure 3 depicts that a rise in variable viscosity parameter increases the velocity profiles. Figure 4 shows that the concentration of nanoparticles in the vicinity of the wall significantly decreases with moving from the wall into the boundary layer. Low values of *Nv* indicates that the viscosity of the nanofluid is highly dependent to the

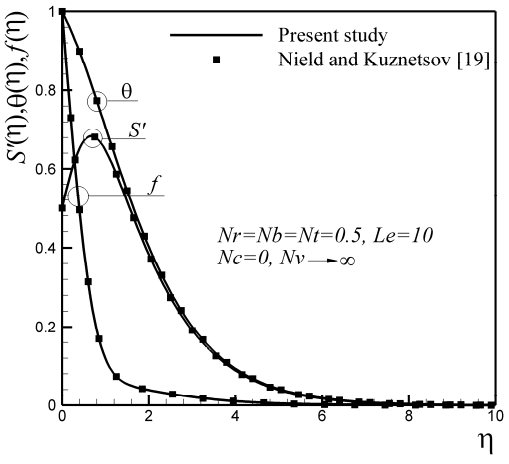

Fig. 2 Comparison of present results with results of Nield and Kuznetsov [19] for temperature, velocity and concentration profiles when $Nc = 0$ and $Nv \to \infty$

https://doi.org/10.1017/jmech.2013.61 Published online by Cambridge University Press

Table 4 Variation of reduced Nusselt number $-\theta'(0)$ and reduced Sherwood number $-f'(0)$ for various values of nanofluid parameters (*Nt*, *Nb* and *Nr*) and variable parameters (*Nc* and *Nv*) for two values of *Le*

Nt	*Nb*	*Nr*	*Nc*	*Nv*	$-\theta'(0)$	∞	$-f'(0)$	∞
					Le = 1E + 3	*Le* = 2E + 3	*Le* = 1E + 3	*Le* = 2E + 3
1.0E−06	1.0E−05	1.0E−03	0	2	0.4379	0.4396	14.5928	20.6811
				10	0.4428	0.4431	17.1597	24.3089
				20	0.4434	0.4435	17.4518	24.7217
				200	0.4440	0.4440	17.7102	25.0869
				$\to\infty$	0.4440	0.4440	17.7329	25.1191
Nt	*Nb*	*Nr*	*Nv*	*Nc*	*Le* = 1E + 3	*Le* = 2E + 3	*Le* = 1E + 3	*Le* = 2E + 3
1.0E−05	1.0E−04	1.0E−03	$\to\infty$	0	0.4438	0.4438	17.7330	25.1191
				0.25	0.3569	0.3564	17.7515	25.1377
				0.5	0.2986	0.2978	17.7645	25.1508
				1	0.2253	0.2243	17.7818	25.1679
Nb	*Nr*	*Nc*	*Nv*	*Nt*	*Le* = 1E + 3	*Le* = 2E + 3	*Le* = 1E + 3	*Le* = 2E + 3
1.0E−04	1.0E−02	0	$\to\infty$	1.0E−09	0.4437	0.4438	17.6831	25.0487
				1.0E−08	0.4437	0.4438	17.6830	25.0475
				1.0E−07	0.4437	0.4438	17.6830	25.0475
				1.0E−06	0.4437	0.4438	17.6829	25.0474
				1.0E−05	0.4437	0.4438	17.6658	25.0352
Nt	*Nr*	*Nc*	*Nv*	*Nb*	*Le* = 1E + 3	*Le* = 2E + 3	*Le* = 1E + 3	*Le* = 2E + 3
1.0E−06	1.0E−02	0	$\to\infty$	1.0E−08	0.4436	0.4437	15.9542	23.8143
				1.0E−07	0.4438	0.4438	17.5101	24.9241
				1.0E−06	0.4438	0.4438	17.6657	25.0351
				1.0E−05	0.4437	0.4438	17.6829	25.0474
Nt	*Nb*	*Nc*	*Nv*	*Nr*	*Le* = 1E + 3	*Le* = 2E + 3	*Le* = 1E + 3	*Le* = 2E + 3
1.0E−06	1.0E−05	0	$\to\infty$	1.0E−05	0.4439	0.4439	17.7387	25.1283
				1.0E−04	0.4439	0.4439	17.7381	25.1264
				1.0E−03	0.4439	0.4439	17.7329	25.1191
				1.0E−02	0.4438	0.4438	17.6813	25.0462
				1.0E−01	0.4429	0.4431	17.1555	24.3047

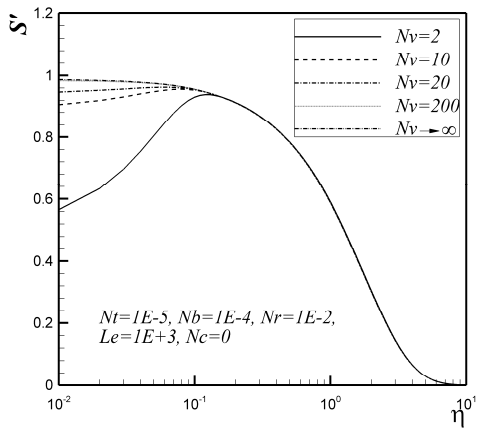

Fig. 3 Velocity profiles for various values of variable viscosity parameter (*Nv*)

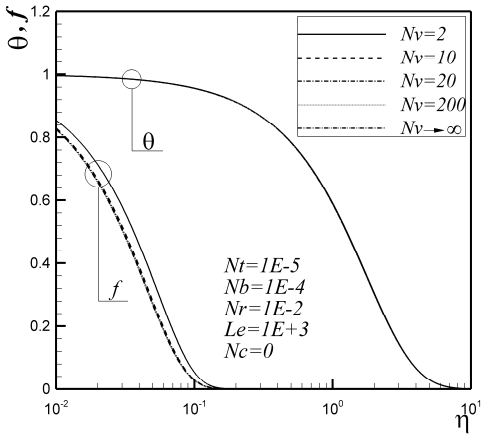

Fig. 4 Temperature and concentration profiles for various values of variable viscosity parameter (*Nv*)

https://doi.org/10.1017/jmech.2013.61 Published online by Cambridge University Press

local concentration. Therefore, the results of Fig. 3 in agreement with the concentration gradient (observed in Fig. 4) show that the velocity profiles are affected by *Nv* in the vicinity of the plate. However, in the areas comparatively far from the wall but inside the hydrodynamic boundary layer, the concentration reaches to the constant value of φ_∞, and variation of viscosity parameter (*Nv*) does not show significant effect on the velocity profiles. As seen in Fig. 3, when the variable viscosity parameter is comparatively low (*Nv* = 2), the velocity profile in the vicinity of the wall is obviously lower than the case of constant viscosity ($Nv \to \infty$). A reason for this behavior is that decreasing the variable viscosity parameter (as seen in Fig. 4) would tend to increase the concentration of nanofluid in the vicinity of the wall. The presence of heavy nanoparticles decreases the buoyancy force near the wall; consequently it decreases the velocity profiles. Simultaneously, decrease of velocity leads to increase of concentration profiles. Figure 4 interestingly reveals that an increase of variable viscosity parameter does not show significant effect on the temperature profiles. Considering Eq. (26a), it can be concluded that $\theta = (Nv / (Nv - f)) \times S' + Nr \times f$. Hence, by the decrease of *f* and increase of *S* ', which were observed by increase of *Nv* in Figs. 3 and 4, the temperature profiles tend to remain constant. Furthermore, the minimum value of dimensionless concentration occurs in the case of constant variable viscosity parameter ($Nv \to \infty$) as seen in Fig. 4. Therefore, the model of constant thermo-physical properties, *i.e.* constant thermal conductivity and constant viscosity, overestimates the velocity profiles and underestimates the concentration profiles.

The non-dimensional profiles of velocity, temperature and concentration are shown in Fig. 5 for different values of variable thermal conductivity parameter (*Nc*). High values of *Nc* denote that the thermal conductivity is highly dependent on local nanoparticles concentration, and zero value of *Nc* denotes that the thermal conductivity is independent of the local nanoparticle concentration. As mentioned earlier, the results show that the thickness of concentration boundary layer is thin in comparison with thickness of the hydrodynamic and thermal boundary layers. This is because of the high values of Lewis number. Lewis number ($\alpha_m / \varepsilon D_B$) shows the ratio of the diffusion of heat (thermal diffusivity) to diffusion of nanoparticles (Brownian diffusivity). Hence, for high values of Lewis number, the thickness of thermal boundary layer is much higher than concentration boundary layer. Therefore, the results are illustrated in the logarithmic scale to obviously display the influence of variable thermal conductivity parameter on the boundary layers. In addition, the results show that the increase of variable thermal conductivity parameter increases the magnitude of velocity and temperature profiles. A reason for this behavior is that an increase of *Nc* would increase the thermal conductivity of the nanofluid near the wall where the local concentration of nanoparticles is comparatively high; thereby, the temperature profiles would increase. Increase of temperature increases the buoyancy force and consequently increases the velocity profiles. As mentioned before, Eq. (26a) shows that there is an obvious relation between temperature, velocity and concentration profiles. Therefore, by simultaneous increase of temperature and velocity profiles, the concentration profiles tend to remain constant which can be seen in Fig. 5. In a comparatively wide region far from the wall but inside the hydrodynamic boundary layer, the concentration tends to the fixed value of φ_∞, and variation of *Nc* has not any significant influence on the velocity and temperature profiles.

As shown in Fig. 5, the increase of thermal conductivity parameter does not show significant effect on the magnitude of concentration profiles.

Figures 6 and 7 show the variation of reduced Nusselt and Sherwood numbers as a function of variable viscosity parameter (*Nv*) and variable thermal conductivity (*Nc*), respectively. These figures depict that increase of variable viscosity parameter increases the magnitude of reduced Nusselt and Sherwood numbers. However, the increase of reduced Nusselt number is negligible. By decreasing the variable viscosity parameter, nanofluid would act as a fluid with high

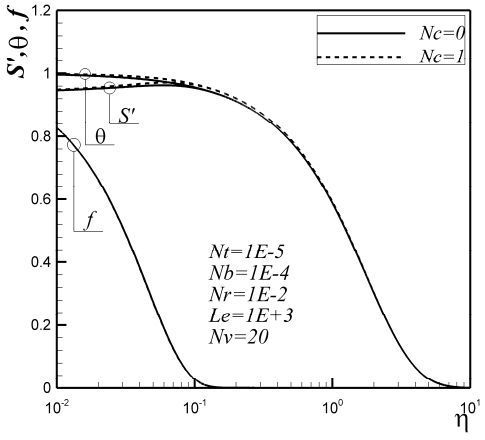

Fig. 5 Velocity, temperature and concentration profiles for various values of variable thermal conductivity parameter (*Nc*)

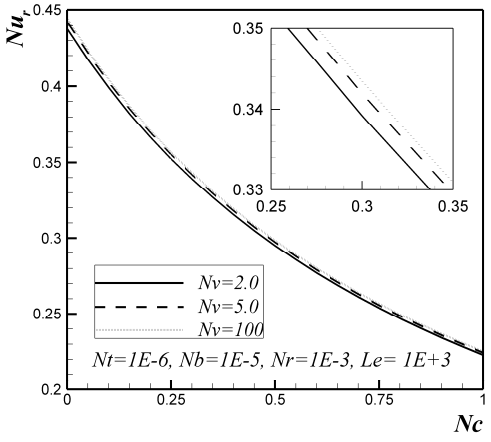

Fig. 6 Reduced Nusselt number profiles for various values of variable viscosity (*Nv)* and variable conductivity (*Nc)* parameters; the small figure shows a magnified view of the curves

https://doi.org/10.1017/jmech.2013.61 Published online by Cambridge University Press

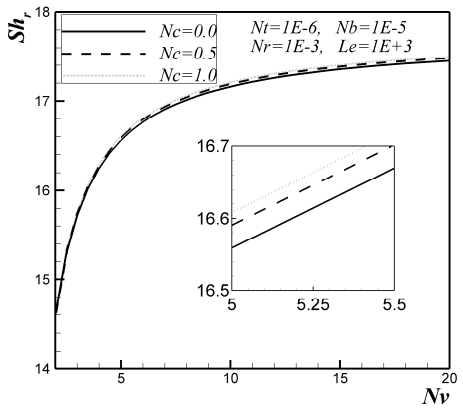

Fig. 7 Reduced Sherwood number profiles for various values of variable viscosity (*Nv)* and variable conductivity (*Nc)* parameters; the small figure shows a magnified view of the curves

viscosity in the vicinity of the wall where the local concentration of nanoparticles in the nanofluid is high. Hence, the velocity of nanofluid would decrease; that in turn it decreases the heat transfer rate (Nu_r). In the Figs. 7 and 8 the curves are close together; therefore a magnified view of the curves is provided inside the figures. Figure 7 illustrates that the increase of variable viscosity parameter increases the magnitude of concentration gradient on the wall surface. This result is in agreement with the results of Fig. 4 and Table 4.

Figures 6 and 7 also depict that an increase of variable conductivity parameter decreases the magnitude of reduced Nusselt number while it increases the magnitude of reduced Sherwood number. However, the augmentation of reduced Sherwood number is not significant. As mentioned, the increase of variable thermal conductivity parameter increases thermal conductivity coefficient near the wall where the local concentration of nanoparticles is high, and thus, the gradient of temperature profiles decreases. It is worth mentioning that based on Eq. (27), $h_x = -k_{m,w}\ \theta'(0)x^{-1}Ra_x^{1/2}$, and hence, the local heat transfer coefficient of natural convection (h_x) not only is a function of reduced Nusselt number but also thermal conductivity. Therefore, the increase of *Nc*, which would simultaneously decrease Nu_r and increase the thermal conductivity on the wall, produces two opposite effects on the heat transfer coefficient (h_x). Recalling Eq. (11), thermal conductivity at the wall is $k_{m,w} = k_{m,\infty} \times (1 + Nc)$. Therefore, considering $Nc = 0$ results in $h_x = 0.4438k_{m,\infty}x^{-1}Ra_x^{1/2}$ and considering $Nc = 1$ results in $0.4506k_{m,\infty}x^{-1}Ra_x^{1/2}$. In summary, it can be concluded that the increase of *Nc* increases the local heat transfer coefficient of natural convection (h_x) for very high values of variable thermal conductivity parameter.

5. CONCLUSIONS

A combined similarity and numerical approach is adopted to theoretically investigate the effect of variable viscosity and thermal conductivity parameters on the natural convection heat transfer from a vertical plate embedded in a porous medium saturated with a nanofluid. In the modeling of nanofluid, the dynamic effects of nanoparticles, thermophoresis and Brownian motion, have been taken into account. Considering six different types of nanofluids, the practical range of nanofluid parameters has been revealed. The effects of variable viscosity and thermal conductivity parameters on the velocity, temperature and concentration profiles, as well as reduced Nusselt and Sherwood numbers, are analyzed. The results of present study can be summarized as follows:

1. The physical range of nanofluid parameters, which has been used by many of previous researchers, is not in good agreement with the practical range of these parameters.
2. Using practical range of non-dimensional parameters demonstrate that the heat transfer associated with migration of nanoparticles is negligible compared with heat transfer associated with conduction and convection. Therefore, contrary to what is commonly stated in the literatures, the nanoparticles indeed affect convective heat transfer in the nanofluids only by affecting the thermo-physical properties. However, the thermal conductivity and viscosity are strongly dependent on the concentration of nanoparticles. Therefore, the concentration gradient can significantly influence the local values of thermal conductivity and viscosity.
3. Increase of variable viscosity parameter increases the velocity profiles whereas decreases the concentration profiles. Moreover, variation of viscosity parameter does not show significant effect on the temperature profiles.
4. As variable viscosity parameter increases, the magnitude of reduced Nusselt and Sherwood numbers would also increase.
5. Increase of variable thermal conductivity parameter increases the velocity and temperature profiles, but it does not show significant effect on the concentration profiles.
6. Increasing the variable thermal conductivity parameter decreases the reduced Nusselt number whereas increases the reduced Sherwood number.

In summary, it can be concluded that the concentration gradient of nanoparticles (because of thermophoresis and Brownian motion forces) affects the local viscosity and thermal conductivity of nanofluids and consequently heat transfer of nanofluids. Hence, the advantage and disadvantage of these effects should be considered in future engineering designs. Some new experimental tests also are needed.

ACKNOWLEDGMENTS

The authors are grateful to Shahid Chamran University of Ahvaz for its crucial support.

NOMENCLATURES

D_B Brownian diffusion coefficient

D_T thermophoretic diffusion coefficient

https://doi.org/10.1017/jmech.2013.61 Published online by Cambridge University Press

f	rescaled nano particle volume fraction, nano particle concentration
g	gravitational acceleration vector
K	permeability of porous medium
k	thermal conductivity
k_m	effective thermal conductivity of the porous medium
h	local heat transfer coefficient of natural convection
Le	Lewis number
m_μ	proportionality coefficient of viscosity
m_k	proportionality coefficient of thermal conductivity
Nb	Brownian motion parameter
Nc	variable thermal conductivity parameter
Nr	buoyancy ratio
Nt	thermophoresis parameter
Nv	variable viscosity parameter
P	pressure
Ra_x	local Rayleigh number
S	dimensionless stream function
T	temperature
T_∞	ambient temperature
T_W	wall temperature of the vertical plate
U	reference velocity
u, v	Darcy velocity components
(x, y)	Cartesian coordinates

Greek Symbols

$(\rho c)_f$	heat capacity of the fluid
$(\rho c)_m$	effective heat capacity of porous medium
$(\rho c)_p$	effective heat capacity of nano particle material
μ	viscosity of fluid
α_m	thermal diffusivity of porous media
β	volumetric expansion coefficient of fluid
ε	porosity
η	dimensionless distance
θ	dimensionless temperature
ρ_f	fluid density
ρ_p	nano particle mass density
τ	parameter defined by Eq. (5)
γ	proportionality coefficient
φ	nano particle volume fraction
φ_∞	ambient nano particle volume fraction
φ_r	constant defined by Eq. (10)
φ_w	nano particle volume fraction at the wall of the vertical plate
ψ	stream function

REFERENCES

1. Das, S. K., Choi, S. U. S., Yu, W. and Pradeep, T., *Nanofluids — Science and Technology*, John Wiley & Sons Publishers, Hoboken (2007).
2. Khanafer, K., Vafai, K. and Lightstone, M., "Buoyancy-Driven Heat Transfer Enhancement in a Two-Dimensional Enclosure Utilizing Nanofluids," *International Journal of Heat and Mass Transfer*, **46**, pp. 3639–3653 (2003).
3. Hwang, K. S., Jang, S. P. and Choi, S. U. S., "Flow and Convective Heat Transfer Characteristics of Water-Based Al_2O_3 Nanofluids in Fully Developed Laminar Flow Regime," *International Journal of Heat and Mass Transfer*, **52**, pp. 193–199 (2009).
4. Yu, W., France, D. M. and Routbort, J. L., "Review and Comparison of Nanofluid Thermal Conductivity and Heat Transfer Enhancements," *Heat Transfer Engineering*, **29**, pp. 432–460 (2008).
5. Daungthongsuk, W. and Wongwises, S., "A Critical Review of Convective Heat Transfer of Nanofluids," *Renewable and Sustainable Energy Reviews*, **11**, pp. 797–817 (2007).
6. Wang, X-Q. and Mujumdar, A. S., "A Review on Nanofluids — Part I: Theoretical and Numerical Investigations," *Brazilian Journal of Chemical Engineering*, **25**, pp. 613–630 (2008).
7. Wang, X-Q, and Mujumdar, A. S., "A Review on Nanofluids — Part II: Experiments and Applications," *Brazilian Journal of Chemical Engineering*, **25**, pp. 631–648 (2008).
8. Kakaç, S. and Pramuanjaroenkij, A., "Review of Convective Heat Transfer Enhancement with Nanofluids," *International Journal of Heat and Mass Transfer*, **52**, pp. 3187–3196 (2009).
9. Nield, D. A. and Bejan, A., *Convection in Porous Media*, 3rd Edition, Springer, New York (2006).
10. Ingham, D. B. and Pop, I., *Transport Phenomena in Porous Media*, Elsevier, Oxford (2005).
11. Vafai, K., *Handbook of Porous Media*, 2nd Edition, Taylor & Francis, New York (2005).
12. Vadasz, P., *Emerging Topics in Heat and Mass Transfer in Porous Media*, Springer, New York (2008).
13. Gorla, R. S. R., Chamkha, A. J. and Rashad, A. M., "Mixed Convective Boundary Layer Flow over a Vertical Wedge Embedded in a Porous Medium Saturated with a Nanofluid-Natural Convection Dominated Regime," *Nanoscale Research Letters*, **6**, pp. 1–9 (2011).
14. Cheng, P. and Minkowycz, W. J., "Free Convection About a Vertical Flat Plate Embedded in a Saturated Porous Medium with Applications to Heat Transfer from a Dike," *Journal of Geophysical Research*, **82**, pp. 2040–2044 (1977).
15. Gorla, R. S. R. and Zinolabedini, "Free Convection from a Vertical Plate with Non Uniform Surface Temperature and Embedded in a Porous Medium," *Journal of Energy Resources Technology*, **109**, pp. 26–30 (1987).

https://doi.org/10.1017/jmech.2013.61 Published online by Cambridge University Press

16. Joshi, Y. and Gebhart, B., "Mixed Convection in Porous Media Adjacent to a Vertical Uniform Heat Flux Surface," *International Journal of Heat and Mass Transfer*, **28**, pp. 1783–1786 (1985).
17. Belhachmi, Z., Brighi, B., Sac-Epee, J. M. and Taous, K., "Numerical Simulations of Free Convection About a Vertical Flat Plate Embedded in a Porous Medium," *Computational Geosciences*, **7**, pp. 137–166 (2003).
18. Buongiorno, J., "Convective Transport in Nanofluids," *Journal of Heat Transfer*, **128**, pp. 240–250 (2006).
19. Nield, D. A. and Kuznetsov, A. V., "The Cheng-Minkowycz Problem for Natural Convective Boundary-Layer Flow in a Porous Medium Saturated by a Nanofluid," *International Journal of Heat and Mass Transfer*, **52**, pp. 5792–5795 (2009).
20. Chamkha, A., Gorla, R. S. R. and Ghodeswar, K., "Non-Similar Solution for Natural Convective Boundary Layer Flow over a Sphere Embedded in a Porous Medium Saturated with a Nanofluid," *Transport in Porous Media*, **86**, pp. 13–22 (2011).
21. Rashad, A. M., El-Hakiem, M. A. and Abdou, M. M. M., "Natural Convection Boundary Layer of a Non-Newtonian Fluid About a Permeable Vertical Cone Embedded in a Porous Medium Saturated with a Nanofluid," *Computers & Mathematics with Applications*, **62**, pp. 3140–3151 (2011).
22. Gorla, R. S. R. and Chamkha, A., "Natural Convective Boundary Layer Flow over a Horizontal Plate Embedded in a Porous Medium Saturated with a Nanofluid," *Journal of Modern Physics*, **2**, pp. 62–71 (2011).
23. Khanafer, K. and Vafai, K., "A Critical Synthesis of Thermophysical Characteristics of Nanofluids," *International Journal of Heat and Mass Transfer*, **54**, pp. 4410–4428 (2011).
24. Chandrasekar, M. and Suresh, S., "A Review on the Mechanisms of Heat Transport in Nanofluids," *Heat Transfer Engineering*, **30**, pp. 1136–1150 (2009).
25. Chin, K. E., Nazar, R., Arifin, N. M. and Pop, I., "Effect of Variable Viscosity on Mixed Convection Boundary Layer Flow over a Vertical Surface Embedded in a Porous Medium," *International communications in Heat and Mass Transfer*, **34**, pp. 464–473 (2007).
26. Kumari, M., "Effect of Variable Viscosity on Non-Darcy Free or Mixed Convection Flow on a Horizontal Surface in a Saturated Porous Medium," *International Communications in Heat and Mass Transfer*, **28**, pp. 723–732 (2001).
27. Hossain, M. A., Munir, M. S. and Pop, I., "Natural Convection Flow of Viscous Fluid with Viscosity Inversely Proportional to Linear Function of Temperature from a Vertical Cone," *International Journal of Thermal Sciences*, **40**, pp. 366–371 (2001).
28. Shit, G. C. and Haldar, R., "Effects of Thermal Radiation on MHD Viscous Fluid Flow and Heat Transfer over Nonlinear Shrinking Porous Sheet," *Applied Mathematics and Mechanics*, **32**, pp. 677–688 (2011).
29. Prasad, K. V., Dulal Pal, V., Umesh, N. S. and Rao, P., "The Effect of Variable Viscosity on MHD Viscoelastic Fluid Flow and Heat Transfer over a Stretching Sheet," *Communications in Nonlinear Science and Numerical Simulation*, **15**, pp. 331–344 (2010).
30. Chaim, T. C., "Heat Transfer with Variable Thermal Conductivity in a Stagnation-Point Flow Towards a Stretching Sheet," *International Communications in Heat and Mass Transfer*, **23**, pp. 239–248 (1996).
31. Hwang, K. S., Jang, S. P. and Choi, S. U. S., "Flow and Convective Heat Transfer Characteristics of Water-Based Al2O3 Nanofluids in Fully Developed Laminar Flow Regime," *International Journal of Heat and Mass Transfer*, **52**, pp. 193–199 (2009).
32. Oztop, H. F. and Abu-Nada, E., "Numerical Study of Natural Convection in Partially Heated Rectangular Enclosures Filled with Nanofluids," *International Journal of Heat and Mass Transfer*, **29**, pp. 1326–1336 (2008).
33. Ma, K.-Q. and Liu, J., "Nano Liquid-Metal Fluid as Ultimate Coolant," *Physics Letters*, **361**, pp. 252–256 (2007).
34. Nassan, T. H., Zeinali Heris, S. and Noie, S. H., "A Comparison of Experimental Heat Transfer Characteristics for Al2O3/Water and Cuo/Water Nanofluids in Square Cross-Section Duct," *International Communications in Heat and Mass Transfer*, **37**, pp. 924–928 (2010).

(Manuscript received February 4, 2013,
accepted for publication May 7, 2013.)

https://doi.org/10.1017/jmech.2013.61 Published online by Cambridge University Press